J|A|C|S
ARTICLES

Published on Web 03/06/2009

Gas-Phase IR Spectroscopy of Deprotonated Amino Acids

Jos Oomens,* Jeffrey D. Steill, and Britta Redlich

FOM Institute for Plasma Physics "Rijnhuizen", Edisonbaan 14, 3439MN Nieuwegein, The Netherlands

Received September 25, 2008; E-mail: joso@rijnhuizen.nl

Abstract: Gas-phase infrared multiple photon dissociation (IRMPD) spectra have been recorded for the conjugate bases of a series of amino acids (Asp, Cys, Glu, Phe, Ser, Trp, Tyr). The spectra are dominated by strong symmetric and antisymmetric carboxylate stretching modes around 1300 and 1600 cm^{-1}, respectively. Comparison of the experimental spectra with spectra calculated at the DFT level suggests a carboxylate structure for all species investigated, which is in contrast with what has recently been suggested in this journal for deprotonated cysteine [*J. Am. Chem. Soc.* **2007**, *129*, 5403−5407]. In addition, the IR spectrum of the conjugate base of tyrosine is also unambiguously that of a carboxylate ion and not that of a phenoxide ion. In sharp contrast with the conjugate bases of other amino acids investigated here, the aspartate and glutamate anions show very broad, hardly resolved spectral features. We present qualitative experimental evidence indicating that this can be attributed to the formation of a proton bridge between the backbone and side chain carboxylate groups. The large amplitude motion of this shared proton, coupling to virtually all other vibrational modes, causes extensive spectral broadening.

Introduction

The application of infrared (IR) spectroscopy to mass-selected molecular ions has resolved various structural questions in mass spectrometry in recent years.[1−4] Particularly for molecules of fundamental biological importance, the use of IR spectroscopy has been able to answer questions that had remained under debate for many years using mass spectrometric methods alone. This is mainly due to the sensitivity of vibrational frequencies to the electron density in bonds involving N and O atoms, which is strongly influenced by hydrogen bonds or metal ion binding, which in turn are crucial to the molecular structure. The site of protonation is a recurring question in experiments involving electrospray ionization that is now being addressed with IR spectroscopy.[5−10] Starting with the work of Ohanessian and coworkers,[11] the structure of a large number of amino acid−alkali metal cation complexes has unambiguously been identified as either charge solvated (canonical) or salt bridge (zwitterion).[12−18] It has recently been confirmed experimentally that a divalent alkaline earth metal cation (Ba^{2+}) forms solely salt bridge structures with most amino acids.[19,20] The site of post-translational modifications in peptides, in particular phosphorylation, has been identified by IR spectroscopy.[10] Of fundamental importance to peptide sequencing in MS, *b*-type fragments in collision-induced dissociation (CID) were spectroscopically confirmed to have an oxazolone structure,[21] and *c*-type fragments resulting from electron capture dissociation (ECD) were shown to have an amide structure.[22] Spectroscopic investigation of the changes in the structure of biomolecular ions upon attachment of one or more water molecules directly

(1) Duncan, M. A. *Int. J. Mass Spectrom.* **2000**, *200*, 545–589.
(2) Oomens, J.; Sartakov, B. G.; Meijer, G.; von Helden, G. *Int. J. Mass Spectrom.* **2006**, *254*, 1–19.
(3) MacAleese, L.; Maitre, P. *Mass Spectrom. Rev.* **2007**, *26*, 583–605.
(4) Asmis, K. R.; Sauer, J. *Mass Spectrom. Rev.* **2007**, *26*, 542–562.
(5) Oh, H. B.; Lin, C.; Hwang, H. Y.; Zhai, H.; Breuker, K.; Zabrouskov, V.; Carpenter, B. K.; McLafferty, F. W. *J. Am. Chem. Soc.* **2005**, *127*, 4076–4083.
(6) Lucas, B.; Gregoire, G.; Lemaire, J.; Maitre, P.; Ortega, J. M.; Rupenyan, A.; Reimann, B.; Schermann, J. P.; Defrancois, C. *Phys. Chem. Chem. Phys.* **2004**, *6*, 2659–2663.
(7) Gregoire, G.; Gaigeot, M. P.; Marinica, D. C.; Lemaire, J.; Schermann, J. P.; Desfrancois, C. *Phys. Chem. Chem. Phys.* **2007**, *9*, 3082–3097.
(8) Polfer, N. C.; Oomens, J.; Suhai, S.; Paizs, B. *J. Am. Chem. Soc.* **2007**, *129*, 5887–5897.
(9) Lucas, B.; Gregoire, G.; Lemaire, J.; Maitre, P.; Glotin, F.; Schermann, J. P.; Desfrancois, C. *Int. J. Mass Spectrom.* **2005**, *243*, 105–113.
(10) Correia, C. F.; Balaj, P. O.; Scuderi, D.; Maitre, P.; Ohanessian, G. *J. Am. Chem. Soc.* **2008**, *130*, 3359–3370.
(11) Kapota, C.; Lemaire, J.; Maitre, P.; Ohanessian, G. *J. Am. Chem. Soc.* **2004**, *126*, 1836–1842.
(12) Polfer, N. C.; Paizs, B.; Snoek, L. C.; Compagnon, I.; Suhai, S.; Meijer, G.; von Helden, G.; Oomens, J. *J. Am. Chem. Soc.* **2005**, *127*, 8571–8579.
(13) Polfer, N. C.; Oomens, J.; Dunbar, R. C. *Phys. Chem. Chem. Phys.* **2006**, *8*, 2744–2751.
(14) Armentrout, P. B.; Rodgers, M. T.; Oomens, J.; Steill, J. D. *J. Phys. Chem. A* **2008**, *112*, 2248–2257.
(15) Rodgers, M. T.; Armentrout, P. B.; Oomens, J.; Steill, J. D. *J. Phys. Chem. A* **2008**, *112*, 2258–2267.
(16) Forbes, M. W.; Bush, M. F.; Polfer, N. C.; Oomens, J.; Dunbar, R. C.; Williams, E. R.; Jockusch, R. A. *J. Phys. Chem. A* **2007**, *111*, 11759–11770.
(17) Bush, M. F.; Forbes, M. W.; Jockusch, R. A.; Oomens, J.; Polfer, N. C.; Saykally, R. J.; Williams, E. R. *J. Phys. Chem. A* **2007**, *111*, 7753–7760.
(18) Bush, M. F.; O'Brien, J. T.; Prell, J. S.; Saykally, R. J.; Williams, E. R. *J. Am. Chem. Soc.* **2007**, *129*, 1612–1622.
(19) Dunbar, R. C.; Polfer, N. C.; Oomens, J. *J. Am. Chem. Soc.* **2007**, *129*, 14562–14563.
(20) Bush, M. F.; Oomens, J.; Saykally, R. J.; Williams, E. R. *J. Am. Chem. Soc.* **2008**, *130*, 6463–6471.
(21) Polfer, N. C.; Oomens, J.; Suhai, S.; Paizs, B. *J. Am. Chem. Soc.* **2005**, *127*, 17154–17155.
(22) Frison, G.; van der Rest, G.; Turecek, F.; Besson, T.; Lemaire, J.; Maitre, P.; Chamot-Rooke, J. *J. Am. Chem. Soc.*, **2008**, *130*, 14916−14917.

10.1021/ja807615v CCC: $40.75

links gas-phase and condensed-phase structures.[18,23] IR spectroscopy revealed that gas-phase H/D exchange can induce structural changes of the analyte molecule.[24] Sophisticated double resonance methods have also been applied to obtain conformer-specific spectra from a heterogeneous sample of cold gas-phase biomolecular ions.[25,26]

Virtually all ions of biological interest investigated with IR spectroscopy to date are cationized species. Although IR spectroscopy has been applied to mass-selected anions previously,[27−33] only very few studies involving negatively charged biomolecules have been reported.[34,35] Here, we present the application of gas-phase IR spectroscopy to deprotonated amino acids.

Though seemingly simple species, fundamental questions regarding the gas-phase structure of deprotonated amino acids remain unanswered to date. Most importantly, the site of deprotonation has been assumed to be the C-terminus for all amino acids,[36] but recently this has been cast in doubt for the conjugate bases of cysteine and tyrosine.[37−40] The situation has been compared to that of the conjugate base of *p*-hydroxybenzoic acid in the gas phase, for which the alcohol group was determined to be deprotonated rather than the carboxylic acid group more than 30 years ago.[41] However, although mass spectrometric methods have been very successfully applied to determine gas-phase acidities, the site of deprotonation and hence the structure of the resulting conjugate base is not as easily determined (see, for example, the discussion in ref 42).

For deprotonated cysteine, the photoelectron spectrum revealed a slightly lower electron binding energy as compared to other deprotonated amino acids.[37] Calculations of the structures of $[Cys - H]^-$ as well as $[Tyr - H]^-$ suggest that deprotonation occurs at the side chain rather than at the C-terminus,[40] and this was supported for Cys by measurements of the gas-phase acidities and by H/D exchange experiments.[38] The conjugate base of cysteine would thus have a thiolate structure and that of tyrosine a phenoxide structure rather than a carboxylate structure. However, the computed thermochemical differences are small, which is for instance reflected in recent experiments using chemical probing where the structure of the conjugate base of Tyr was found to depend on the solvent used in the electrospray ionization source.[39] Hence, it is clear that further experimental verification of amino acid anion structures is highly desirable, and here we present infrared spectra for the conjugate bases of Phe, Trp, Tyr, Cys, Asp, Glu, and Ser. Except for the acidic amino acids, the IR spectra provide an unambiguous structural characterization, which, perhaps surprisingly, suggest that all deprotonated amino acids have a carboxylate structure in the gas phase.

The carbonyl stretch of a carboxylic acid moiety is one of the most significant bands in the IR spectra of organic acids, including amino acids. Upon deprotonation, a carboxylate moiety is formed, which also has a very diagnostic infrared fingerprint: the symmetric and antisymmetric OCO stretch modes, which are extremely sensitive to the environment particularly as a consequence of the delocalized electron wave function. These modes, and in particular their separation, have therefore been widely used in condensed-phase spectroscopic studies to determine the coordination mode in carboxylate salts and solutions.[43−45] The first gas-phase spectrum of a carboxylate anion has recently been recorded for the benzoate anion.[46] The separation between symmetric and antisymmetric OCO stretch modes is roughly doubled compared to condensed-phase spectra, demonstrating the extreme sensitivity of the carboxylate modes to the (absence of the) environment.

Experimental Section

Infrared spectra are obtained by IRMPD spectroscopy of the anions mass selectively isolated in a Fourier transform ion cyclotron resonance (FTICR) mass spectrometer. Intense and tunable IR radiation is generated by the FELIX free electron laser at our institute.[47] In the wavelength range applied here (800−1800 cm^{-1}), the pulse energy amounts to around 50 mJ per 5-μs pulse, while the bandwidth is on the order of 0.5% of the central wavelength. Although an IRMPD spectrum relies on a mechanism that is different from a direct absorption spectrum, the IRMPD spectrum usually represents a good approximation to the linear spectrum.[2]

Deprotonated amino acid anions are generated by electrospray ionization (ESI) of an approximately 1 mM solution of the amino acid in an 80/20 mixture of methanol and water with typically 2 mM of base (usually NaOH) added to assist deprotonation. The ESI source is a slightly adapted Micromass Z-Spray source, where the rf hexapole ion guide is used as an accumulation trap. Ions are typically accumulated for several seconds before being pulse extracted from the trap into the ICR cell via a 1-m long rf octopole ion guide.

In the ICR cell, the parent ions are SWIFT isolated by *m*/*z* and irradiated with typically about 12 FEL pulses. After irradiation, a

(23) Kamariotis, A.; Boyarkin, O. V.; Mercier, S. R.; Beck, R. D.; Bush, M. F.; Williams, E. R.; Rizzo, T. R. *J. Am. Chem. Soc.* **2006**, *128*, 905–916.
(24) Polfer, N. C.; Dunbar, R. C.; Oomens, J. *J. Am. Soc. Mass Spectrom.* **2007**, *18*, 512–516.
(25) Stearns, J. A.; Mercier, S. R.; Seaiby, C.; Guidi, M.; Boyarkin, O. V.; Rizzo, T. R. *J. Am. Chem. Soc.* **2007**, *129*, 11814–11820.
(26) Stearns, J. A.; Boyarkin, O. V.; Rizzo, T. R. *J. Am. Chem. Soc.* **2007**, *129*, 13820–13821.
(27) Shin, S. K.; Beauchamp, J. L. *J. Am. Chem. Soc.* **1990**, *112*, 2066–2069.
(28) Wild, D. A.; Bieske, E. J. *Int. Rev. Phys. Chem.* **2003**, *22*, 129–151.
(29) Pivonka, N. L.; Kaposta, C.; von Helden, G.; Meijer, G.; Wöste, L.; Neumark, D. M.; Asmis, K. R. *J. Chem. Phys.* **2002**, *117*, 6493–6499.
(30) Bopp, J. C.; Roscioli, J. R.; Johnson, M. A. *J. Phys. Chem. A* **2007**, *111*, 1214–1221.
(31) Groenewold, G. S.; Oomens, J.; de Jong, W. A.; Gresham, G. L.; McIllwain, M. E.; van Stipdonk, M. J. *Phys. Chem. Chem. Phys.* **2008**, *10*, 1192–1202.
(32) Choi, J.; Kuwata, K. T.; Cao, Y. B.; Okumura, M. *J. Phys. Chem. A* **1998**, *102*, 503–507.
(33) Cabarcos, O. M.; Weinheimer, C. J.; Lisy, J. M.; Xantheas, S. S. *J. Chem. Phys.* **1999**, *110*, 5–8.
(34) Chiavarino, B.; Crestoni, M. E.; Fornarini, S.; Lanucara, F.; Lemaire, J.; Maitre, P.; Scuderi, D. *Int. J. Mass Spectrom.* **2008**, *270*, 111–117.
(35) Gabelica, V.; Rosu, F.; de Pauw, E.; Lemaire, J.; Gillet, J.-C.; Poully, J.-C.; Lecomte, F.; Gregoire, G.; Schermann, J. P.; Defrancois, C. *J. Am. Chem. Soc.* **2008**, *130*, 1810–1811.
(36) O'Hair, R. A. J.; Bowie, J. H.; Gronert, S. *Int. J. Mass Spectrom. Ion Processes* **1992**, *117*, 23–36.
(37) Woo, H. K.; Lau, K. C.; Wang, X. B.; Wang, L. S. *J. Phys. Chem. A* **2006**, *110*, 12603–12606.
(38) Tian, Z.; Pawlow, A.; Poutsma, J. C.; Kass, S. R. *J. Am. Chem. Soc.* **2007**, *129*, 5403–5407.
(39) Tian, Z.; Kass, S. R. *J. Am. Chem. Soc.* **2008**, *130*, 10842–10843.
(40) Jones, C. M.; Bernier, M.; Carson, E.; Colyer, K. E.; Metz, R.; Pawlow, A.; Wischow, E. D.; Webb, I.; Andriole, E. J.; Poutsma, J. C. *Int. J. Mass Spectrom.* **2007**, *267*, 54–62.
(41) McMahon, T. B.; Kebarle, P. *J. Am. Chem. Soc.* **1977**, *99*, 2222–2230.
(42) Bartmess, J. E.; Scott, J. A.; McIver, R. T. *J. Am. Chem. Soc.* **1979**, *101*, 6046–6056.
(43) Deacon, G. B.; Phillips, R. J. *Coord. Chem. Rev.* **1980**, *33*, 227–250.
(44) Nara, M.; Torii, H.; Tasumi, M. *J. Phys. Chem. A* **1996**, *100*, 19812–19817.
(45) Lewandowski, W.; Kalinowska, M.; Lewandowska, H. *J. Inorg. Biochem.* **2005**, *99*, 1407–1423.
(46) Oomens, J.; Steill, J. D. *J. Phys. Chem. A* **2008**, *112*, 3281–3283.
(47) Oepts, D.; van der Meer, A. F. G.; van Amersfoort, P. W. *Infrared Phys. Technol.* **1995**, *36*, 297–308.

Table 1. Observed IRMPD Dissociation Channels and Their (presumable) Identification[a]

$[AA - H]^-$	parent mass	fragment mass	
Trp	203	159	CO_2 loss
		116	$[indole - H]^-$
Phe	164	147	**NH_3 loss**
		103	
		46	
Tyr	180	163	NH_3 loss
		119	$CH_2{=}CH{-}C_6H_4O^-$
		136	CO_2 loss
		93	$C_6H_5O^-$
		72	$HN{=}CH{-}COO^-$
Cys	120	33	**HS^-**
Ser	104	74	**CH_2O loss**
Asp	132	115	NH_3 loss
		88	**CO_2 loss**
		114	**H_2O loss**
Glu	146	128	**H_2O loss**
		102	**CO_2 loss**

[a] Fragments observed by Bowie and co-workers[49] in CAD mass spectra are in boldface.

mass spectrum is generated using an excite/detect sequence as implemented in the FTICR control software, which is an adapted version of that described by Heeren and co-workers.[48] At each wavelength, three mass spectra are averaged and the parent and fragment ion intensities are used to determine the percentile fragment yield $Y = \sum I_f/(I_p + \sum I_f)$, where I_p and I_f are the integrated intensities of the mass peaks of the parent and fragment ions. The yield is then plotted as a function of wavelength to obtain the IRMPD spectrum. Using irradiation time and intensity, the fragmentation yield was typically kept below 50% to avoid saturation effects.

The experimental spectra are compared to calculated spectra to identify the molecular structures. The lowest energy structures of the deprotonated forms of all twenty naturally occurring amino acids have recently been calculated by Poutsma and co-workers.[40] Unless otherwise noted, we use these structures and the Gaussian03 software package to perform a frequency calculation (after optimization) at the density functional level of theory using the B3LYP functional and the 6−31++G** basis set, which was recently found to be adequate to reproduce the spectra of gaseous (substituted) benzoate anions.[46] The vibrational frequencies in the 600−1800 cm^{-1} wavelength range are scaled by a uniform factor of 0.98. For comparison with the experimental spectra, the computed vibrational frequencies are convoluted with a 20 cm^{-1} fwhm Gaussian line shape.

Results and Discussion

Mass Spectra. The fragmentation pathways observed upon IRMPD are listed in Table 1 and can be compared to results from collisionally activated dissociation (CAD) that have been reported[49] for some of the deprotonated amino acids studied here. In general, the main fragmentation pathways are similar to those observed by CAD, although many of the minor channels are not observed under our conditions, likely because of a lower internal energy and a narrower internal energy distribution. For Asp, Cys, Glu, and Ser, all fragmentation channels observed here have been identified by CAD (see bold entries in Table 1). For Phe, the main channel, NH_3 loss, corresponds to the CAD mass spectrum, but in addition we observe fragment peaks at *m/z* 103 and 46. Trp and Tyr were not reported by Bowie and co-workers.[49] Identification of these fragment channels is therefore less secure. The loss of a neutral CO_2 unit has been observed as the main IRMPD fragmentation channel for several benzoate derivatives[46] and is also abundantly observed for Trp and Tyr.

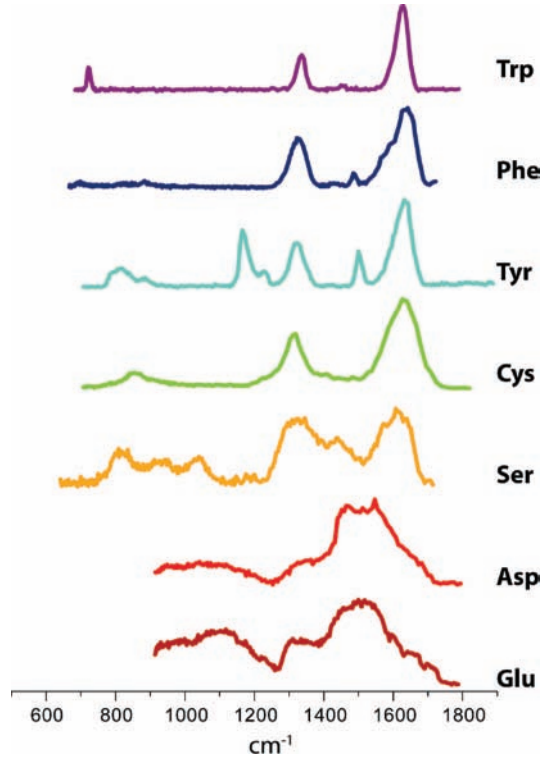

Figure 1. Experimental gas-phase IRMPD spectra of the conjugate bases of the amino acids investigated in this study and listed by their three-letter code on the right. While all spectra were recorded under similar conditions, the resolution in the spectra appears to deteriorate roughly going from side chains with an aromatic ring to those with a heteroatom, to those with a carboxylic acid.

The identification of the fragmentation products is in fact irrelevant for the IR spectra to be obtained, and we will not analyze the fragmentation pathways in further detail. To generate an IRMPD spectrum, the fragment intensities in all channels are summed and divided by the total ion intensity (parent + fragments). This total fragment yield is then plotted as a function of the wavelength of the incident radiation, giving the IRMPD spectra shown in Figure 1.

Tryptophan. The IRMPD spectrum of the deprotonated Trp anion shown in Figure 2 is very sparse, especially considering that this is the largest species in the data set. The symmetric (1337 cm^{-1}) and antisymmetric (1628 cm^{-1}) carboxylate stretching modes are the main features of the spectrum. The match with the spectrum calculated for the $[Trp - H]^-$ structure of Poutsma and co-workers[40] is very good for these modes. In addition, two weaker features are observed in the IRMPD spectrum, which correspond excellently with the computed spectrum: the out-of-plane CH bending mode of the indole ring at 721 cm^{-1} and the $C_\beta H_2$ scissoring mode at 1457 cm^{-1}.

These four bands matching almost exactly with theory gives good confidence in the computed structure, and the discrepancies between experiment and theory mainly between 900 and 1100 cm^{-1} are therefore all the more mysterious. The three bands in the convoluted theoretical spectrum are in fact made up of four main vibrational modes computed at 928, 998, 1087, and 1097

(48) Mize, T. H.; Taban, I.; Duursma, M.; Seynen, M.; Konijnenburg, M.; Vijftigschild, A.; Doornik, C. V.; Rooij, G. V.; Heeren, R. M. A. *Int. J. Mass Spectrom.* **2004**, *235*, 243–253.
(49) Eckersley, M.; Bowie, J. H.; Hayes, R. N. *Int. J. Mass Spectrom. Ion Processes* **1989**, *93*, 199–213.

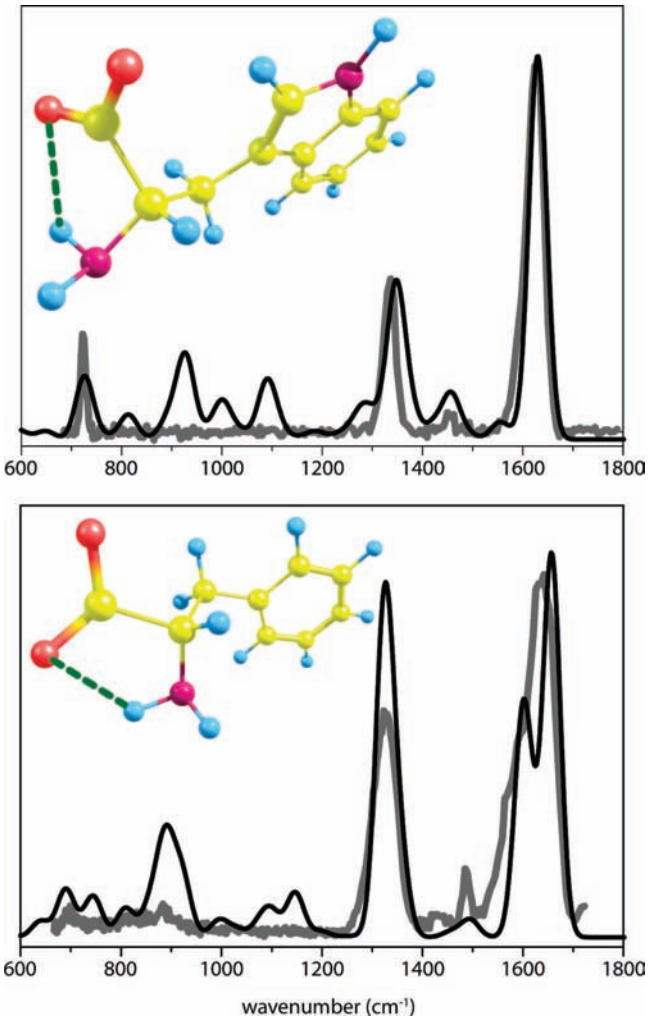

Figure 2. Experimental (gray) and theoretical spectra of the conjugated bases of Trp (top) and Phe (bottom). Calculated spectra are based upon the minimum energy structures taken from ref 40.

cm^{-1}. These unobserved vibrations all have mostly NH_2 wagging character, and such modes are known for their more anharmonic behavior, for instance in the case of aniline.[50] Possibly, the more anharmonic nature of these modes makes the computed frequencies and intensities less reliable and, moreover, may cause the multiple photon excitation process to be less efficient for these modes.

Phenylalanine. For deprotonated amino acids without heteroatoms in the side chain, such as phenylalanine, the number of possible hydrogen-bonding motifs is basically limited to that where one of the hydrogen atoms of the N-terminus interacts with the deprotonated C-terminus. This is indeed the case for the structure reported in ref 40, and a frequency calculation for this structure is compared to the experiment in Figure 2.

The spectrum of deprotonated phenylalanine shows the characteristic symmetric and antisymmetric OCO stretching modes of the carboxylate group near 1330 and 1640 cm^{-1}, respectively. In the high frequency part of the spectrum, two additional bands are discernible: a mode with mainly NH_2 scissoring character appears as a shoulder on the red edge of the main antisymmetric carboxylate stretch band, and a weak feature is observed at 1490 cm^{-1}, which is assigned as a CH in-plane bending mode of the phenyl group.

(50) Sinclair, W. E.; Pratt, D. W. *J. Chem. Phys.* **1996**, *105*, 7942–7956.

Similar to the Trp case, some discrepancies are observed between experimental and calculated spectra in the 1000−1200 cm^{-1} range. In particular, two calculated bands that are due to NH_2 wagging and rocking modes are not observed in the experimental spectrum. Perhaps the low intensity in combination with a possibly higher anharmonicity precludes the observation of these bands in the IRMPD spectrum. In the long wavelength range, a reasonable match between experiment and theory is obtained in terms of band positions, although the observed intensities appear to be substantially lower than predicted. The low photon energy in this spectral range combined with nonlinearities in the multiple photon excitation process may lead to lower observed band intensities. The computations show that the band near 900 cm^{-1} is mainly localized on the amino group and that the band near 700 cm^{-1} is due to the CH out-of-plane mode of the benzyl side chain.

Tyrosine. Compared to the other aromatic amino acids, the conjugate base of tyrosine is an interesting case since two different structures have been proposed. It has been suggested that a phenoxide structure, where the side-chain hydroxyl is deprotonated, is lower in energy than the carboxylate structure, albeit by a small margin.[37−40] This small preference for the phenoxide structure is mainly due to a more favorable hydrogen-bonding network.

IR spectra have been calculated for the two structures at the B3LYP/6−31++G(d,p) level. Despite the slightly lower level of theory employed here, the energy difference between the two structures is the same as that calculated in ref 40. The calculated spectra are compared to the experimental IRMPD spectrum in Figure 3. In contrast to what theory predicts, the experimental spectrum is clearly that of a carboxylate structure. The complete absence of an absorption band higher than 1700 cm^{-1}, where the C═O stretch mode of the carboxylic acid group is predicted for the phenoxide structure, suggests that the phenoxide structure constitutes at most a very minor fraction of the ion population. Instead, a strong band is observed at 1635 cm^{-1}, which is attributed to the asymmetric carboxylate stretch and the NH_2 scissor mode, which appear to be slightly closer in frequency than calculated and therefore not resolved. The remainder of the spectrum, which is significantly richer than those of the other aromatic amino acid anions, matches excellently with that computed for the carboxylate structure. Of interest are the band at 1164 cm^{-1}, which is assigned as the hydroxyl COH bending mode, and the feature around 1325 cm^{-1}, which is mainly due to the symmetric carboxylate stretching mode. These bands provide further compelling evidence for a purely carboxylate structure of the $[Tyr - H]^-$ anion, despite the phenoxide structure being calculated to be lower in energy at the present level of theory. Only the band calculated at 910 cm^{-1}, which is due to an NH_2 wagging mode, appears to be weaker and slightly red-shifted in the experimental spectrum.

Tian and Kass[39] recently claimed that the actual structure of $[Tyr - H]^-$ present in the gas phase depends on the solvents used in the electrospray ionization of the anions. When methanol is used as a solvent, the anion is suggested to convert from its carboxylate structure in solution to a phenoxide structure once in the gas phase. Using an aprotic solvent such as acetonitrile was found to result in a carboxylate gas-phase structure. In contrast, our experiments find a purely carboxylate gas-phase structure while using an ESI solution containing 75% methanol.

One possible caveat of IRMPD spectroscopy on anions is further explored here. Upon multiple-photon excitation, the anions may not only undergo dissociation but also detachment.

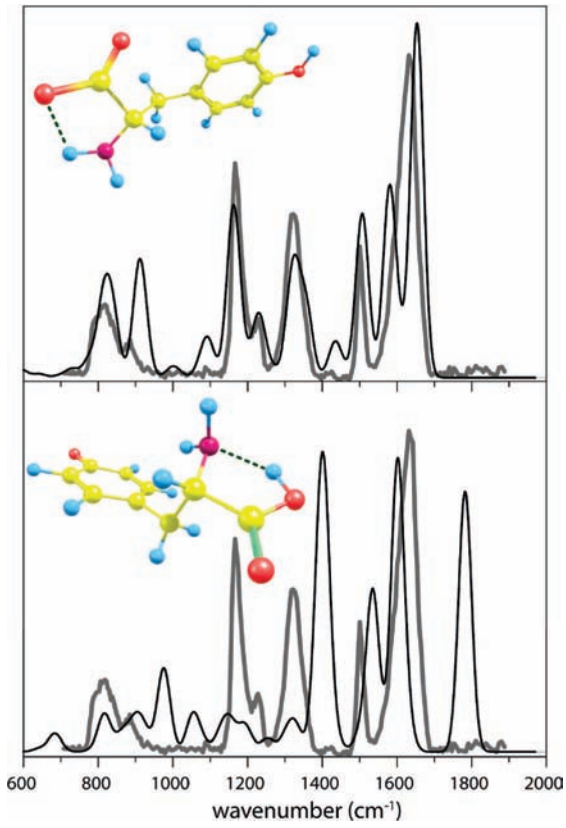

Figure 3. Experimental IRMPD spectrum of deprotonated Tyr (gray) compared to theoretical spectra for the carboxylate (top) and phenoxide (bottom) forms of the anion. Structures are taken from ref 40 and optimized at the B3LYP/6−31++G** level. The IRMPD spectrum is clearly that of a carboxylate structure; the absence of any significant intensity around 1800 cm^{-1} excludes the phenoxide structure.

In contrast to dissociation, electron detachment is not directly observable in the FTICR mass spectrum because the electron mass cannot be detected. Thus, if a phenoxide structure would, in contrast to a carboxylate structure, undergo only detachment upon IR irradiation, it could be present in our mass spectrometer but have escaped from observation. In order to verify this possibility, we applied a slightly different form of action spectroscopy based on detachment and subsequent electron capture by an electron scavenger, as we have recently described elsewhere.[51] Here, $[Tyr - H]^-$ is irradiated in the ICR cell in the presence of a partial pressure of about 5E-8 Torr of neutral SF_6. Electrons detached after multiple photon excitation are thus captured and detected as SF_6^- in the mass spectrum. The IR spectrum recorded via detachment is shown in Figure S1 of the Supporting Information and peak positions are virtually the same as those recorded via IRMPD; again, there is no intensity observed around 1800 cm^{-1} again suggesting that the phenoxide structure is not present. The detachment spectrum mirrors the dissociation spectrum closely, indicating that all ions in the population have a carboxylate structure and that detachment and dissociation are two competing processes under these irradiation conditions.

Cysteine. Recent investigations into the gas-phase acidities of the 20 natural amino acids have suggested that the thiol group in cysteine may be more acidic than the backbone carboxylic acid.[40] For the conjugate base of cysteine, the thiolate structure was found to be 13.8 kJ/mol lower in free energy than the lowest energy carboxylate structure, based on calculations performed at the B3LYP/aug-cc-pVDZ level of theory.[38] Experimental results, in particular H/D exchange and kinetic method measurements, indicate that the acidities of the carboxylic acid and thiol groups are at least very similar.[38] Moreover, Woo et al.[37] find evidence for a thiolate structure in their photoelectron spectra of deprotonated cysteine and some derivatives. In their studies, Kass, Poutsma, and co-workers consider various possible structures for the deprotonated cysteine anion (see Chart 1), which can roughly be divided into thiolates and carboxylates, although proton-sharing between the carboxylate and thiolate groups occurs to some degree in structures **2** and **3**.

Here we have performed frequency calculations for the four lowest energy structures found in refs 38 and 40. The relative energy ordering does not change at the slightly lower level of theory used here. A comparison of the calculated spectra with the experimental spectrum is shown in Figure 4. Surprisingly, the IRMPD spectrum does not match with the spectrum calculated for the lowest energy isomer, which has a thiolate structure (referred to as structure **3** in ref 38). A good spectral match is however found with the lowest energy carboxylate structure (structure **1**), which is predicted to be higher in energy by 13.8 kJ/mol.[38]

The strongest band in the spectrum is observed at approximately 1630 cm^{-1} and must correspond to a CO stretch in either a carboxylate or thiolate structure. The thiolate structures **3** and **4** have a protonated carboxylate, i.e., a carboxylic acid with a C═O moiety (see Chart 1). Indeed, the calculated CO stretches for structures **3** and **4** occur at higher frequencies than those of the carboxylate structures **1** and **2**. The CO stretch mode of **4** is significantly blue-shifted relative to that of **3**, where the CO is involved in a hydrogen bond with the N-terminus in contrast to **4**, which possesses a free carbonyl. In any case, the CO stretch modes of both structures are clearly higher in frequency than that in the experimental spectrum. The carboxylate structures **1** and **2**, on the other hand, show a good match with the observed 1630 cm^{-1} band. In our recent study of gas-phase carboxylate ions,[46] the asymmetric OCO stretch of the benzoate anion was observed at 1626 cm^{-1}, very close to the band observed here for the deprotonated cysteine anion.

The next strongest band in the experimental spectrum is observed at 1315 cm^{-1}, and it leaves little doubt that this is the symmetric OCO stretching mode of the carboxylate group. In contrast to the calculated carboxylate spectra, the calculated spectra for the two thiolate structures **3** and **4** do not show any significant intensity at this frequency. For the gas-phase benzoate anion and several of its substituted forms,[46] the symmetric OCO stretching mode was observed around 1310 cm^{-1}. In combination with the better overall match of the entire spectrum, this analysis of the CO stretch modes provides compelling evidence for a carboxylate structure of the conjugate base of cysteine.

The symmetric OCO stretching mode around 1315 cm^{-1} as well as the spectrum at longer wavelengths appears to agree better with structure **1** than with structure **2**. The three bands calculated for **1** around 855, 927, and 1010 cm^{-1} correspond to modes localized mostly on the amino group. These modes could smear out to give the observed feature peaking at 855 cm^{-1} and showing a long tail to higher frequencies. Though somewhat tentative, the agreement of the experimental spectrum with the calculations for **1** appears to be substantially better than with those for **2**. In agreement with the calculated free energies,[38] **1** is indeed approximately 4 kJ mol^{-1} more stable than **2**.

(51) Steill, J. D.; Oomens, J. arXiv:0809.2519.

Chart 1. Different H-Bonding Interactions in the Carboxylate (**1**, **2**) and Thiolate (**3**, **4**) Forms of the Conjugate Base of Cysteine[38]

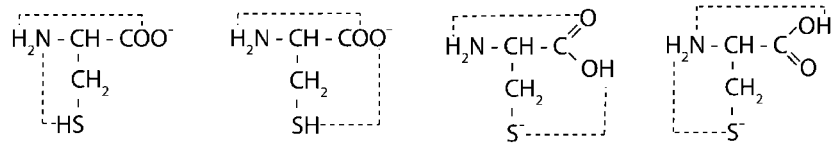

1 **2** **3** **4**

Similar to $[Tyr - H]^-$, the question now remains why we observe the conjugate base of cysteine to be a carboxylate structure, while the thiolate structure is calculated to be more stable by about 13 kJ mol^{-1} at the DFT level of theory.[38] Could multiple photon IR excitation and dissociation be preferentially sensitive to one structure and not to the other? There is no reason to believe that the IR absorption intensities would be radically different, and moreover the barrier to interconversion between the structures is likely lower than the dissociation threshold, so that the accessible dissociation channels are likely independent of the original structure before excitation (see, for example, Figure 13 in ref 18). Furthermore, it is also unlikely that one structure absorbs several laser photons and then isomerizes to another structure which is not resonant with the laser frequency, since this would require the ions to completely recondense into another potential well. At the time scale of an FEL pulse (5 μs) and under the high vacuum conditions of the FTICR-MS, this is unlikely. Rather, upon IR activation, the ion becomes more dynamical and probes a larger proportion of the conformational space, and its spectrum broadens to the extent where absorption is possible at almost any wavelength.[52] Note that the IR absorption nonetheless initiates in the unexcited, room-temperature ion and it is generally assumed that the observed spectrum is determined by these first photons, which form the bottleneck in the process.[2,52] Although in previous experiments, the lowest energy structure is found to match the spectrum in almost all cases[8,11,12,14,15,21,22] and although higher energy structures were mostly observed as minor contributors only,[13,16] there have also been examples of the IRMPD spectrum showing only one structure, where two structures were calculated to be very close in energy.[53] In the case of deprotonated amino acids, there is the additional complication that the carboxylate structures are known to be lower in energy in solution, and the question whether these structures can be transferred to the gas phase and become kinetically trapped is still under much debate, given for instance recent findings for the conjugate base of tyrosine.[39] Such effects are likely strongly dependent on experimental conditions and a spectroscopic investigation of such effects in a classical example anion, the conjugate base of *p*-hydroxybenzoic acid,[41] is currently underway in our laboratory. It is also of interest to note here that we have previously found that gas-phase H/D exchange may produce species trapped in local minima.[24] Finally, the DFT computed energy gap of 13 kJ mol^{-1} is close to the estimated computational accuracy,[38] and further investigation is thus of interest. Tian et al.[38] found that a larger basis set decreased the DFT calculated gap to 8.4 kJ mol^{-1}, but high-level ab initio calculations (G3B3) gave a slightly larger gap of 13 kJ mol^{-1}. Woo et al.[37] reported a ZPE corrected energy gap of 6.8 kJ mol^{-1} at the B3LYP level and of 9.6 kJ mol^{-1} at the CCSD(T) level. From an experimental point of view, spectra in the hydrogen stretching range, e.g., using OPO sources, may shed further light on this issue, as the spectra are predicted to be very different for thiolate and carboxylate structures (see Supporting Information).

Glutamic and Aspartic Acid. Aspartic and glutamic acid both contain a carboxylic acid moiety in their side chain. Compared to the other deprotonated amino acids presented in this work, the spectra of the aspartate and glutamate anions appear quite different (see also Figure 1). Individual vibrational bands are hardly distinguishable, and the spectra merely show a few unresolved 'blobs'. Moreover, vibrational frequencies calculated for the minimum energy structures[40] do not match the broad and unresolved features observed, as shown in Figure 5.

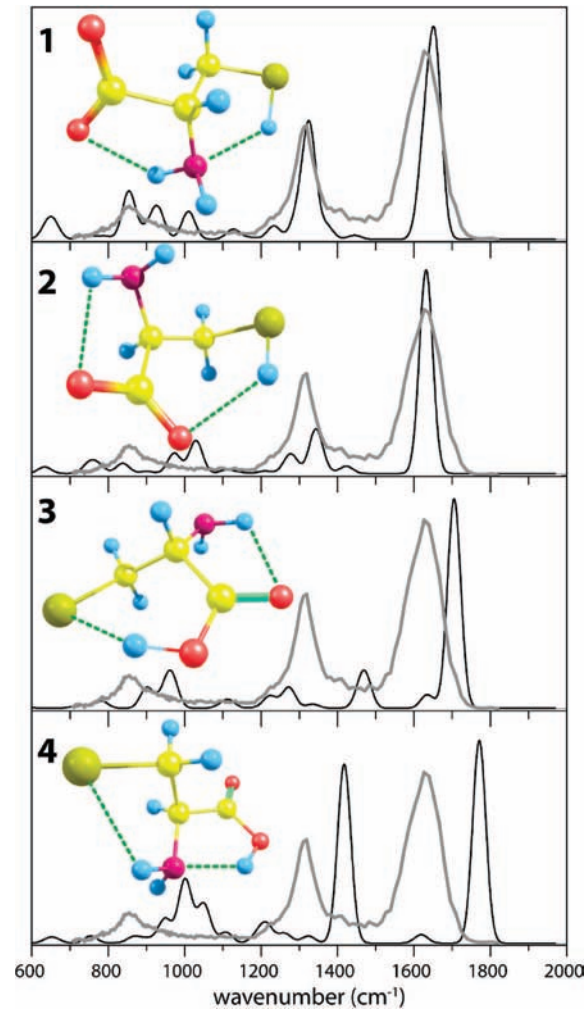

Figure 4. Experimental spectrum of the conjugate base of Cys (gray in all four panels) compared to DFT calculated spectra for structures **1**−**4** of Poutsma and co-workers.[40] Although the thiolate structure **3** is calculated to be lowest in energy, the experimental spectrum shows the best match with a carboxylate structure, particularly structure **1**.

(52) Bagratashvili, V. N.; Letokhov, V. S.; Makarov, A. A.; Ryabov, E. A. *Multiple Photon Infrared Laser Photophysics and Photochemistry*; Harwood: Chur, Switzerland, 1985.
(53) Oomens, J.; Moore, D. T.; Meijer, G.; von Helden, G.; Dunbar, R. C. *J. Am. Chem. Soc.* **2004**, *126*, 724–725.

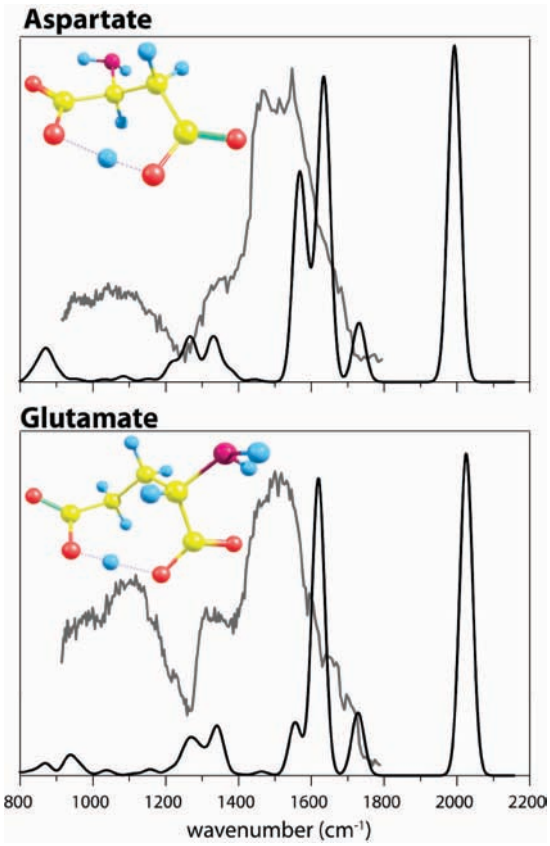

Figure 5. IRMPD spectra observed for the glutamate and aspartate anions (gray) compared to harmonic frequency calculations (black) of the lowest energy structures.[40]

For both bases, theory predicts a structure in which a proton bridge is formed between two carboxylate groups.[40] The harmonic spectra calculated for these structures are dominated by a strong band just higher than 2000 cm^{-1}, which is due to the $O\cdots H^+\cdots O$ stretch mode. Although it seems unfortunate that this band falls just outside the FELIX scan range chosen for these experiments, the band is not actually expected to be found here due to its very anharmonic nature and the fact that this mode has been observed at much lower frequencies in related systems (vide infra). Next lower in frequency in the calculated spectra are three bands which are due to the $O\cdots H^+\cdots O$ bending mode, the NH_2 bending mode, and the carboxylate stretching mode. If these three modes correspond to the most intense feature observed in the experimental spectra, a red-shift of approximately 100 cm^{-1} with respect to the calculated spectra has to be accounted for. The agreement of the remainder of the spectrum is possibly even worse, and in conclusion, one must simply face that harmonic frequency calculations are unable to explain the gas-phase IRMPD spectra of glutamate and aspartate.

Previously, IRMPD spectra have been reported for species with a proton shared between two neutral oxygen atoms,[54−57] the most famous example being undoubtedly the protonated water dimer.[54] A general feature of these IRMPD spectra is the relatively broad spectral resonances, as compared to species not containing an $O\cdots H^+\cdots O$ moiety. Shared proton binding motifs are classified as strong hydrogen bonds when the distance between the heavy atoms is less than approximately 2.5 Å and as intermediate when it is less than ∼2.8 Å. As the distance between the oxygen atoms decreases, the potential energy barrier between the two positions for the proton becomes progressively lower and eventually drops below the zero-point energy; the proton can then move freely between the two positions. On average, the delocalized proton assumes a position symmetrical between the two O-atoms.

Situations where the proton is shared between two negatively charged heteroatoms are well-known examples of low-barrier, strong hydrogen bonds. Some of these systems have even been spectroscopically investigated in the gas phase, such as bihalide anions (XHX^-)[29,58,59] and the hydrated hydroxide ion ($H_3O_2^-$).[60,61] In the latter system,[61] the stretching mode of the proton was identified at 670 cm^{-1}, lower than in any of the overall cationic species, which range from 3300 cm^{-1} (close to a free OH stretch) to about 1000 cm^{-1}, depending on the degree of delocalization.[62] The present case, where a proton is shared between two negatively charged carboxylate groups, appears as an intermediate case between the heteroatoms being neutral and negatively charged. Theory predicts the distance between the two carboxylate oxygen atoms sharing the proton to be slightly less than 2.5 Å, i.e., in the regime where the proton is delocalized between the two positions.

The fact that the proton moves in a very anharmonic potential has a large impact on the infrared spectrum and the ability of harmonic frequency calculations to correctly predict the spectrum. Instead of being close to harmonic, the potential energy surface experienced by the shared proton is relatively flat in the middle and the proton can undergo large amplitude motions between the two heavy atoms. Moreover, the anharmonic nature of the vibrational modes involving the shared proton causes them to couple easily to other vibrational modes of the molecule.

Systems containing a shared proton investigated at low temperatures in a molecular beam using Ar predissociation spectroscopy, a linear absorption technique, show well resolved spectra.[62,63] Recent ab initio molecular dynamics simulations[64] indeed suggest that the spectral broadening observed in IRMPD spectra can be attributed to a combination of mode couplings and higher temperatures, i.e., room temperature, prevalent in these experiments. Such calculations have been able to reconcile the differences in the spectra observed using IRMPD spectroscopy and vibrational predissociation spectroscopy. The extensive coupling of the shared proton vibrations and backbone vibrations call for full-dimensional quantum-chemical computations, which

(54) Asmis, K. R.; Pivonka, N. L.; Santambrogio, G.; Brümmer, M.; Kaposta, C.; Neumark, D. M.; Wöste, L. *Science* **2003**, *299*, 1375–1377.
(55) Moore, D. T.; Oomens, J.; van der Meer, L.; von Helden, G.; Meijer, G.; Valle, J.; Marshall, A. G.; Eyler, J. R. *Chem. Phys. Chem.* **2004**, *5*, 740–743.
(56) Fridgen, T. D.; McMahon, T. B.; MacAleese, L.; Lemaire, J.; Maitre, P. *J. Phys. Chem. A* **2004**, *108*, 9008–9010.
(57) Fridgen, T. D.; MacAleese, L.; Maitre, P.; McMahon, T. B.; Boissel, P.; Lemaire, J. *Phys. Chem. Chem. Phys.* **2005**, *7*, 2747–2755.
(58) Kawaguchi, K.; Hirota, E. *J. Chem. Phys.* **1987**, *87*, 6838–6841.
(59) Pivonka, N. L.; Kaposta, C.; Brümmer, M.; Von Helden, G.; Meijer, G.; Wöste, L.; Neumark, D. M.; Asmis, K. R. *J. Chem. Phys.* **2003**, *118*, 5275–5278.
(60) Diken, E. G.; Headrick, J. M.; Roscioli, J. R.; Bopp, J. C.; Johnson, M. A.; McCoy, A. B.; Huang, X.; Carter, S.; Bowman, J. M. *J. Phys. Chem. A* **2005**, *109*, 571–575.
(61) Diken, E. G.; Headrick, J. M.; Roscioli, J. R.; Bopp, J. C.; Johnson, M. A.; McCoy, A. B. *J. Phys. Chem. A* **2005**, *109*, 1487–1490.
(62) Roscioli, J. R.; McCunn, L. R.; Johnson, M. A. *Science* **2007**, *316*, 249–254.
(63) Headrick, J. M.; Bopp, J. C.; Johnson, M. A. *J. Chem. Phys.* **2004**, *121*, 11523–11526.
(64) Li, X.; Moore, D. T.; Iyengar, S. *J. Chem. Phys.* **2008**, *128*, 184308.

Chart 2. Terephthalate (**5**) and Phthalate (**6**) Anions

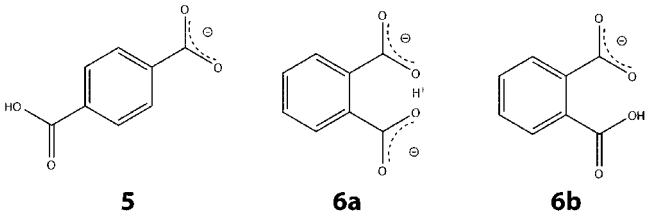

have so far only been carried out for relatively small systems, such as the protonated water dimer.[65]

Although such calculations are unavailable for the glutamate and aspartate anions, we can investigate the phenomenon further experimentally. To this end, we recorded IRMPD spectra of two isomers of the conjugate base of benzenedicarboxylic acid, phthalate and terephthalate (**5** and **6** in Chart 2). Phthalic acid has carboxylic acid groups in the 1 and 2 ring positions, whereas the terephthalic acid isomer has them in the 1 and 4 positions. Theory predicts that the phthalate anion features a proton bridge between two negatively charged carboxylate moieties (**6a**). Phthalate structures in which the proton is not shared (**6b**) optimize to nonplanar structures which are higher in energy by more than 60 kJ mol^{-1}. In contrast to phthalate, interaction between the two carboxylic acid groups cannot occur in the terephthalate isomer, **5**, because of the rigid phenyl ring separating them. Theory therefore predicts an anion with one negatively charged carboxylate group and one neutral carboxylic acid group.

The seemingly small difference between the two isomers has profound effects on the appearance of the IRMPD spectrum and on the ability of harmonic frequency calculations to predict the vibrational spectra (Figure 6). The terephthalate spectrum features well resolved bands matching excellently with DFT calculated harmonic frequencies. Two strong bands in the 1600−1800 cm^{-1} region of the spectrum are assigned as the carboxylic acid C═O stretch (1730 cm^{-1}) and the asymmetric carboxylate OCO stretch (1640 cm^{-1}). The weaker band appearing as a shoulder at 1595 cm^{-1} is due to a ring CC stretch mode, which was also observed in the spectrum of the benzoate anion.[46] The remainder of the spectrum shows the carboxylate symmetric OCO stretch mode at 1296 cm^{-1}, the carboxylic acid COH bending mode at 1165 cm^{-1}, a ring in-plane CH bending mode at 1045 cm^{-1} (which also contains some C−O stretch character), and a more delocalized mode at 740 cm^{-1}, all in excellent agreement with theory.

The phthalate spectrum (Figure 6A), on the other hand, shows much broader resonances, and there is no obvious match with the frequencies calculated for the lowest energy structure featuring a shared proton. Assignment to this structure appears secure though, since the experimental spectrum does not show any absorption higher than 1700 cm^{-1}, indicating that there is no carboxylic acid C═O and hence directly supporting the proton-bridged structure **6a**. We conclude that the broadening of spectral bands as well as the very poor match with computed harmonic frequencies is caused by the shared proton motif probed at room temperature by infrared multiple-photon excitation.

Serine. The lowest energy structure for the conjugate base of serine features a hydrogen bond between the hydroxyl and carboxylate group.[40] One could consider this structure as a

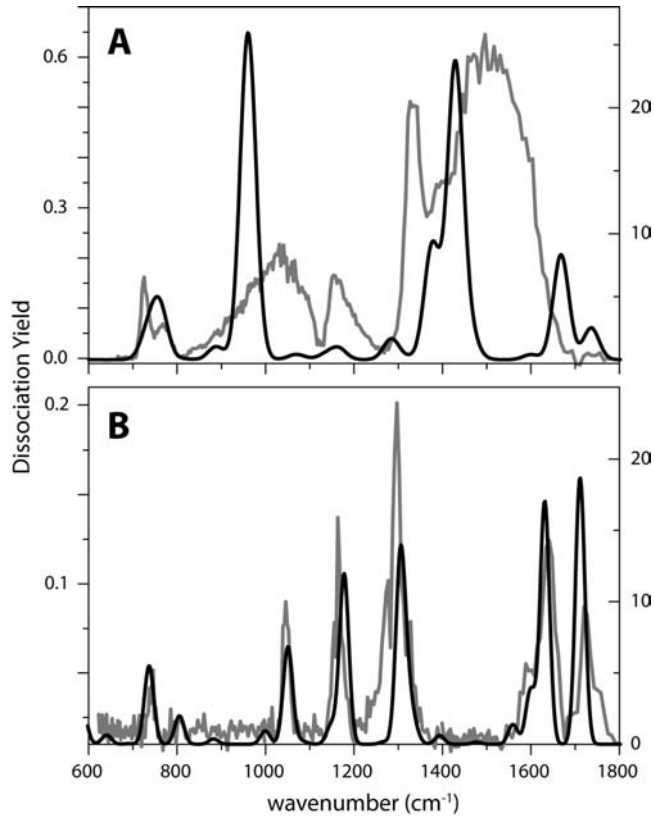

Figure 6. IRMPD spectra of the phthalate (A) and terephthalate (B) anions. The terephthalate spectrum shows well resolved peaks and is in excellent agreement with theory, whereas the phthalate spectrum features much broader absorptions and matches poorly with a harmonic frequency calculation.

proton bridge between negatively charged alkoxide and carboxylate groups. However, the proton is not equally shared as in the case where the proton is delocalized between two carboxylate groups, such as in aspartate and glutamate (vide supra). The potential in which the proton finds itself here is more asymmetric due to the different basicities of the alkoxide and carboxylate groups. With increasing difference in basicity, the potential becomes more asymmetric, localizing the proton to the site with the highest proton affinity. In addition, the potential becomes increasingly more harmonic and the stretching vibration of the proton shifts to higher frequencies, eventually approaching that of a free OH stretching mode. These effects have recently been described in great detail by Johnson and co-workers.[62,66]

Here, the spectrum of the deprotonated serine anion, shown as the gray trace in Figure 7, is observed to be somewhat broadened, though not nearly as much as those of glutamate and aspartate. Moreover, comparison of the experimental spectrum with that calculated for the structure predicted by Poutsma and co-workers[40] (structure **7** in Figure 7) gives a reasonable match. The computed OH stretch frequency is >3000 cm^{-1} (see Table 2), clearly indicating a localized proton[62,66] in contrast to the glutamate and aspartate anions.

Despite the reasonable match displayed in the top panel of Figure 7, some discrepancies are apparent. The intensity of the band marked with an asterisk, identified as the OH bending

(65) McCoy, A. B.; Huang, X.; Carter, S.; Landeweer, M. Y.; Bowman, J. M. *J. Chem. Phys.* **2005**, *122*, 061101.

(66) Roscioli, J. R.; Diken, E. G.; Johnson, M. A.; Horvath, S.; McCoy, A. B. *J. Phys. Chem. A* **2006**, *110*, 4943–4952.

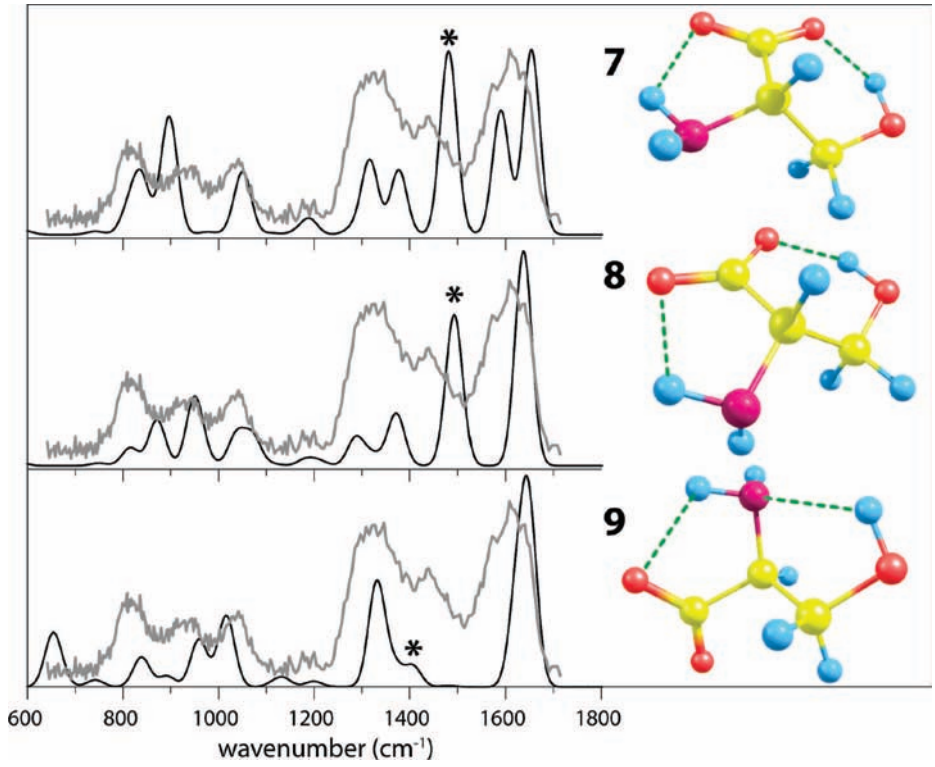

Figure 7. Experimental spectrum of $[Ser - H]^-$ (gray in all panels) compared to computed spectra for three different low-energy structures. Structure (**7**) is that of ref 40. The asterisk indicates the OH bending mode.

Table 2. Low-Energy Structures Computed for the Deprotonated Serine Anion[a]

	7	8	9
H-bonding network	OH···OCO···HNH	OH···OCO···HNH	OH···NH···OCO
ZPE corrected electronic energy (kJ/mol)	+0.24	0	+11.22
free energy at 298 K (kJ/mol)	+0.38	0	+12.76
OH···OCO distance (Å)	1.747	1.705	
OCO···HNH distance (Å)	2.064	2.218	
HCNH dihedral angle	11°	−87°	−29°
OH bend (cm^{-1})[b]	1483	1494	1406
OH stretch (cm^{-1})[c]	3303	3218	3619

[a] Structure **7** corresponds to that of ref 40. [b] Scaled DFT value. [c] Unscaled DFT value.

mode, seems out of proportion, and moreover, its frequency matches quite poorly with the experimentally observed band. Therefore, computed spectra for several other low-energy conformers were generated, which are also shown in Figure 7. Structure **8** is close to **7**, with a similar hydrogen bonding network, but involving the other of the two amino hydrogen atoms, changing mainly the HCNH dihedral angle (see Table 2). Although its energy is virtually the same as that of **7**, the hydrogen bond lengths are different (see Table 2) causing the predicted spectrum to show significant differences. In particular, compared to structure **7** the combined NH_2 scissor and asymmetric OCO stretching modes above 1550 cm^{-1} become unresolved in structure **8**. In addition, the OH bending mode shifts to the blue by about 10 cm^{-1} due to the slightly stronger OH···OCO hydrogen bonding interaction. This shift increases the discrepancy with the experimental spectrum, and in general, structure **8** gives a match with the experiment no better than that of structure **7**. A different hydrogen-bonding network is conceivable as shown by structure **9**. Here, the hydroxyl H-atom interacts with the amino N-atom, giving rise to a weaker hydrogen bond, a longer OH···NH distance, and a substantial redshift of the OH bending mode (see Table 2). Compared to the experimental spectrum, however, this shift appears too large, and moreover, the computed energy of **9** is about 12 kJ/mol higher than that of **7** and **8**. In conclusion, none of the computed spectra match the OH bending mode very well, possibly indicating the more anharmonic nature of this mode. On the basis of computed energies and the general match with the experimental spectrum, also taking into consideration the 600−1000 cm^{-1} range, a structure with an OH···OCO···HNH hydrogen bonding network (**7** and **8**) is the most likely structure of the gas-phase conjugate base of serine, in agreement with the findings of Poutsma and co-workers.[40]

Conclusions

Gas-phase IR spectra for a set of deprotonated amino acid anions have been recorded by IRMPD spectroscopy using a free electron laser coupled to an FTICR mass spectrometer. Comparison of experimental and theoretical spectra, the latter based on the DFT calculated structures of Poutsma and co-workers, provides a structural assignment for the conjugate bases of most amino acids investigated here. Most surprising is perhaps the spectrum of the conjugate base of cysteine, which strongly suggests a carboxylate anion and not a thiolate anion, despite the latter being calculated to be more stable and despite various recent studies reporting a thiolate structure. In addition, the

spectrum of the conjugate base of tyrosine is unambiguously that of a carboxylate structure and not that of a phenoxide structure, whereas the phenoxide is slightly lower in energy and has previously been suggested as the gas-phase structure. These findings from IR spectroscopy suggest that all gas-phase amino acids adopt a carboxylate structure upon deprotonation.

In contrast to the other species studied here, the spectra for the conjugate bases of amino acids with an acidic side chain, i.e., glutamic and aspartic acid, show very broad and unresolved features. The band positions, if recognizable at all, do not seem to correspond with harmonic frequency calculations performed for the reported minimum energy structure. We suggest that this is due to the multiple photon exciation mechanism in combination with the intramolecular proton bridge that is formed between the two carboxylate groups. Previous IRMPD spectra on species possessing a shared proton between two equivalent oxygen atoms tend to show similarly broad spectral features. A comparison between the IRMPD spectra of gas-phase phthalate and terephthalate supports this hypothesis.

Acknowledgment. We gratefully acknowledge the excellent support of Dr. AFG van der Meer as well as others at the FELIX facility. This work is part of the research program of FOM, which is financially supported by the Nederlandse Organisatie voor Wetenschappelijk Onderzoek (NWO).

Supporting Information Available: Figure S1, computed harmonic frequencies for all structures, optimized structures **8** and **9**. This material is available free of charge via the Internet at http://pubs.acs.org.

JA807615V